minutes. The immunoreactive material was eluted in one peak at 26.8% acetonitrile. This peak was then chromatographed on a final RPLC run with 0.1% TFA-acetonitrile as the mobile phase.
14. H. P. J. Bennett, C. A. Browne, S. Solomon, *J. Liq. Chromatogr.* **3**, 1353 (1980).
15. F. Esch *et al.*, *Proc. Natl. Acad. Sci. U.S.A.* **82**, 6507 (1985).
16. P. Böhlen and R. Schroeder, *Anal. Biochem.* **126**, 144 (1982).
17. P. Argos, W. L. Taylor, C. D. Minth, J. E. Dixon, *J. Biol. Chem.* **258**, 8788 (1983).
18. Y. C. Patel, H. H. Zingg, C. B. Srikant, *Adv. Exp. Med. Biol.* **188**, 71 (1985); D. F. Trent and G. C. Weir, *Endocrinology* **108**, 2033 (1981).
19. D. Richter, in *The Posterior Pituitary: Hormone Secretion in Health and Disease*. P. H. Baylis and P. L. Padfield, Eds. (Dekker, New York, 1985), pp. 37–51.
20. R. Newcomb and R. H. Scheller, *J. Neurosci.* 7, 854 (1987).
21. U. Gubler *et al.*, *Proc. Natl. Acad. Sci. U.S.A.* **80**, 4311 (1983).
22. R. J. Deschenes *et al.*, *ibid.* **81**, 726 (1984).
23. R. Guillemin *et al.*, *Science* **218**, 585 (1982); J. Spiess, J. Rivier, W. Vale, *Nature (London)* **303**, 532 (1983).
24. J. Takeda *et al.*, *Endocr. Soc. Abstr.* 1011 (1987); A. Gray, T. J. Dull, A. Ullrich, *Nature (London)* **303**, 724 (1983).
25. T. W. Schwartz, *FEBS Lett.* **200**, 1 (1986).
26. M. Schaefer *et al.*, *Cell* **41**, 457 (1985).
27. H. Matsuo, A. Miyata, K. Mizuno, *Nature (London)* **305**, 721 (1983).
28. G. Thibault *et al.*, *FEBS Lett.* **167**, 352 (1984); M. Yamanaka *et al.*, *Nature (London)* **309**, 719 (1984); M. Maki *et al.*, *ibid*, p. 722; T. G. Flynn, M. L. deBold, A. J. deBold, *Biochem. Biophys. Res. Commun.* **117**, 859 (1983).
29. N. Itoh, K. Obata, N. Yanaihara, H. Okamoto, *Nature (London)* **304**, 547 (1983).
30. K. E. Mayo, G. M. Cerelli, M. G. Rosenfeld, R. M. Evans, *ibid.* **314**, 464 (1985).
31. E. Boel, T. W. Schwartz, K. E. Norris, N. P. Fiil, *EMBO J.* **3**, 909 (1984).
32. We thank R. Guillemin for encouragement, S. Reichlin for reading the manuscript and for useful suggestions, and G. Gravel and R. Schroeder for technical assistance. R.B. was supported by MRC grant MA 9145, by FRSQ and by The Montreal General Hospital Research Institute. N.L. and F.E. were supported by grants HD 09690 and AM I88II.

7 July 1987; accepted 25 September 1987

Synthesis of a Sequence-Specific DNA-Cleaving Peptide

JAMES P. SLUKA, SUZANNA J. HORVATH, MICHAEL F. BRUIST, MELVIN I. SIMON, PETER B. DERVAN

A synthetic 52-residue peptide based on the sequence-specific DNA-binding domain of Hin recombinase (139–190) has been equipped with ethylenediaminetetraacetic acid (EDTA) at the amino terminus. In the presence of Fe(II), this synthetic EDTA-peptide cleaves DNA at Hin recombination sites. The cleavage data reveal that the amino terminus of Hin(139–190) is bound in the minor groove of DNA near the symmetry axis of Hin recombination sites. This work demonstrates the construction of a hybrid peptide combining two functional domains: sequence-specific DNA binding and DNA cleavage.

MANY DNA-BINDING PROTEINS consist of two structural domains each with distinct functions. One domain recognizes and binds a specific DNA sequence, while the other catalyzes a chemical reaction on DNA. A synthetic 52-residue peptide identical to the COOH-terminal domain of Hin recombinase (190 amino acids) has been shown to bind to Hin recombination sites (26 bp) and to inhibit Hin activity (*1*). We now describe the conversion of this sequence-specific DNA-binding peptide into a sequence-specific DNA-cleaving peptide by covalent attachment of an iron chelator, ethylenediaminetetraacetic acid (EDTA), to the NH_2-terminus of the peptide. In the presence of Fe(II), molecular oxygen, and a reducing agent, the synthetic EDTA-peptide oxidatively cleaves DNA at Hin binding sites, revealing the base position and groove location of the NH_2-terminus of the peptide when bound to DNA.

X-ray crystal structures of a number of sequence specific DNA-binding proteins (or fragments) have become available (*2–7*). Comparison of the three-dimensional structures of λ-cro, λ-repressor, and catabolite gene activator protein (CAP) led to the postulate that a conserved α helix–turn–α helix motif is involved in sequence specific DNA recognition (*8, 9*). The crystal structure of a complex formed between the DNA-binding domain of phage 434 repressor (1–69) and a synthetic 434 operator DNA (14 bp) reveals that the peptide, which includes a helix-turn-helix domain, recognizes in DNA both a particular conformation and an array of base-pair contacts (*7*). Helix-turn-helix binding in the major groove of B-DNA may be a common structural feature for sequence-specific DNA affinity (*9, 10*).

Hin recombinase inverts a segment of DNA to change the expression of the flagellin genes of *Salmonella typhimurium* (*11*). Recombination occurs between two crossover sites, designated *hix*L and *hix*R in inverted repeat configuration, when they are on a supercoiled substrate (*12*). Each *hix* site is 26 bp long and has near twofold symmetry. Hin protein binds to a *hix* site as a dimer and protects bases −17 through +16 inclusive. Using solid-phase peptide synthesis, Bruist *et al.* (*1*) prepared a 52–amino acid peptide, identical to the COOH-terminus of Hin(139–190), that constitutes the putative sequence specific DNA-binding domain of Hin. The ability of Hin(139–190) to bind the *hix*L site was demonstrated by deoxyribonuclease (DNase) I and dimethyl sulfate protection experiments (footprinting) (*1*). The synthetic Hin(139–190) protected the same DNA sequence as Hin, except for the central three bases from −2 to +1. For purified Hin(139–190), an apparent dissociation constant of 0.2 μ*M* to *hix*L was determined by DNA mobility retardation assays (*13*).

Attachment of EDTA · Fe(II) to a DNA-binding molecule creates an efficient DNA-cleaving molecule (25°C, *p*H 7.0) (*14*). Attachment of EDTA converts a sequence-specific DNA-binding molecule to a bifunctional molecule capable of binding and cleaving DNA at the recognition site by oxidation of the DNA backbone (*15, 16*). Cleavage is initiated by the addition of a reducing agent such as dithiothreitol (DTT) or sodium ascorbate. Analysis of the cleavage patterns visualized by gel electrophoresis allows both the binding site location and the orientation of the synthetic DNA-binding molecules on double helical DNA to be identified (*15, 16*). Moreover, since the oxidative deoxyribose degradation is mediated by a diffusible species (most likely hydroxyl

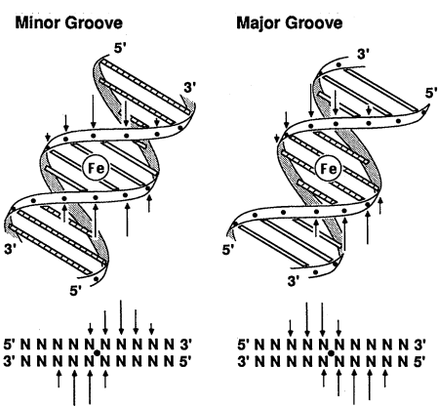

Fig. 1. Cleavage patterns produced by a diffusible oxidant generated by EDTA · Fe localized in the minor and major grooves of right-handed DNA. The edges of the bases are shown as open and crosshatched bars for the minor and major grooves, respectively.

J. P. Sluka and P. B. Dervan, Division of Chemistry and Chemical Engineering, California Institute of Technology, Pasadena, CA 91125.
S. J. Horvath, M. F. Bruist, M. I. Simon, Division of Biology, California Institute of Technology, Pasadena, CA 91125.

radical), the asymmetry of the cleavage patterns on opposite strands of the DNA reveals the identity of the groove in the right-handed helix occupied by the bound EDTA · Fe. An asymmetric cleavage pattern with maximal cleavage shifted to the 5′ or 3′ side on the opposite strands corresponds to the EDTA being positioned in the major or minor groove, respectively (Fig. 1).

To covalently attach EDTA to the NH_2-terminus of the peptide, we prepared a protected EDTA derivative. Three of the carboxyl arms of the EDTA were protected as benzyl esters analogous to the benzyl esters of glutamic and aspartic acids commonly used in the Merrifield solid-phase peptide synthesis (*17*). The fourth carboxyl arm was coupled to a γ-aminobutyric acid (GABA) linker to minimize interference from EDTA · Fe with the secondary or tertiary structure of Hin(139–190). Tribenzyl-EDTA-GABA (BEG) couples to the NH_2-terminus of a protected, resin-bound synthetic peptide. The 52-residue peptide was prepared by stepwise manual solid-phase peptide synthesis (*1*). After terminal *t*-butoxycarbonyl removal, BEG was covalently attached to the resin-bound protected peptide in the presence of *N*,*N*′-dicyclohexylcarbodiimide and *N*-hydroxybenzotriazole (four equivalents of each relative to peptide, 2 m*M* final concentration in dimethylformamide). Quantitative ninhydrin analysis indicated a better than 99% yield for the reaction after 40 hours. Deprotection with anhydrous hydrogen fluoride produced peptide 1 [EDTA-Hin(139–190)], (Fig. 2).

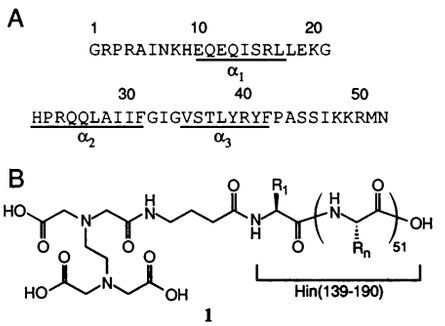

Fig. 2. (**A**) The 52-residue peptide is the COOH-terminus of Hin, amino acids 139 to 190. Tentative α helix assignments are underlined; helices α_2 and α_3 are from alignment with CAP and λ-cro, α_1 was assigned using the Garnier algorithm (*21*). (**B**) Synthetic peptide 1, EDTA-Hin(139–190).

Crude Fe · EDTA-Hin(139–190) at micromolar concentration was allowed to react for 1 hour (22°C, *p*H 7.8) in the presence of DTT with an end-labeled restriction fragment containing the Hin binding sites. This afforded two cleavage loci at *hix*L corresponding to one EDTA-Hin(139–190) per half-site (Fig. 3). Controls showed that neither the 52-residue peptide nor the Hin protein gave detectable DNA cleavage under the same conditions. Equilibration times in the range of 0 to 60 minutes of Fe · EDTA-Hin(139–190) with DNA prior to addition of reducing agent had no effect on cleavage specificity. Fe · EDTA-Hin(139–190) cleavage showed a dependence on salt concentration with 13 times more cleavage in 2 m*M* NaCl than in 400 m*M* NaCl. The EDTA-Hin(139–190) purified by reversed phase high-performance liquid chromatography (HPLC) had the same DNA-cleaving specificity as the crude material but cleaved at tenfold lower concentrations. For comparison with the affini-

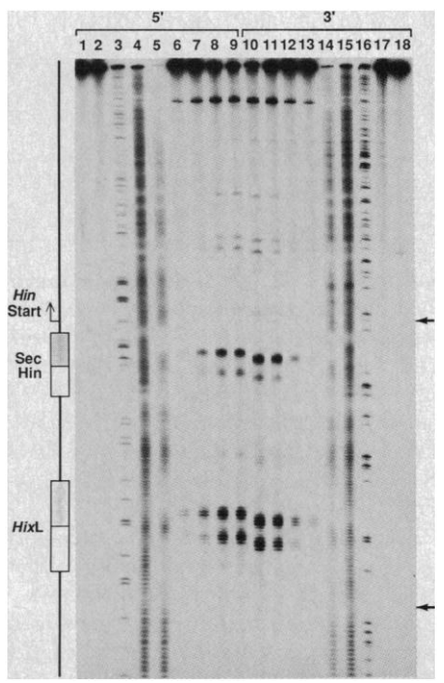

Fig. 3. Autoradiogram of high resolution denaturing gel of Fe · EDTA-Hin(139–190) cleavage of a ^{32}P–end-labeled fragment (Xba I–Eco RI) from pMFB36 (*1*). Reaction conditions were 20 m*M* NaCl, 20 m*M* tris-HCl, *p*H 7.8, 80 μ*M* transfer RNA (tRNA), 5 m*M* DTT, and ≈15,000 cpm (≈1 ng) end-labeled DNA in a total volume of 10 μl. Reactions were run for 40 minutes at 22°C for EDTA-Hin(139–190) and controls, 8 minutes for MPE · Fe footprinting lanes. Cleavage products were analyzed on an 8%, 1 to 20 cross-linked, 50% urea denaturing polyacrylamide wedge gel (0.2 mm thick at the top and 0.6 mm thick at the bottom). (Lanes 1 to 9 and 10 to 18) 5′ and 3′ end-labeled DNA, respectively; (lanes 1 and 18) DNA control; (lanes 2 and 17) minus EDTA controls [10 μ*M* Hin(139–190), 10 μ*M* Fe(II)]; (lanes 3 and 16) Maxam-Gilbert chemical sequencing G lanes; (lanes 4 and 15) MPE · Fe (10 μ*M*) controls; (lanes 5 and 14) MPE · Fe (10 μ*M*) footprints in the presence of Hin(139–190) (10 μ*M*); (lanes 6 and 13) Fe · EDTA-Hin(139–190) at 0.5 μ*M*, (lanes 7 and 12) at 1.5 μ*M*; (lanes 8 and 11) at 5 μ*M*, and (lanes 9 and 10) at 10 μ*M*. Concentrations of EDTA-Hin(139–190) and Hin(139–190) are based on the weight of crude product. The inclusion of a polyanion carrier such as calf-thymus DNA or tRNA reduces the level of nonspecific cleavage. (Left) Marked are *hix*L, the secondary Hin binding site (sec Hin), and start of the *hin* gene (*1*). (Right) Cleavage data between the arrows are shown in Fig. 4.

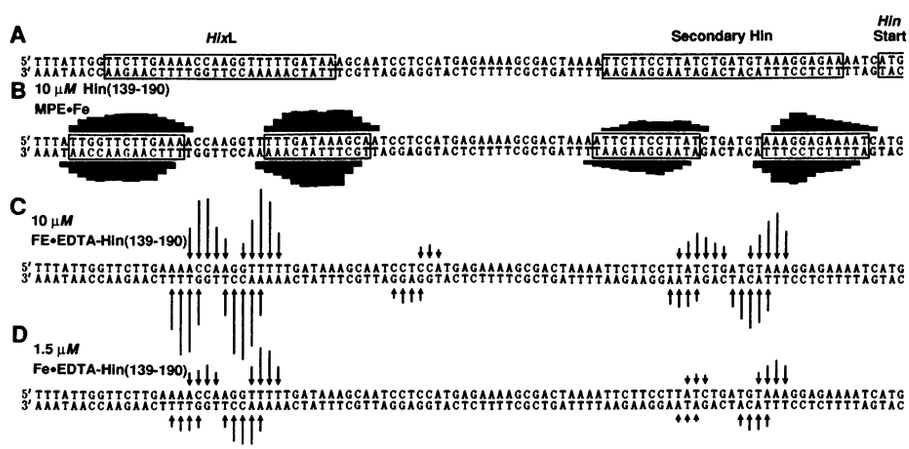

Fig. 4. The sequence left to right represents the cleavage data from the bottom to the middle of the gel in Fig. 3. (**A**) Boxes are the 26-bp *hix*L binding site, secondary Hin-binding site, and start of the *hin* gene. (**B**) Bars represent extent of protection from MPE · Fe cleavage in the presence of Hin(139–190) (Fig. 3, lanes 5 and 14). (**C**) Arrows represent extent of cleavage for Fe · EDTA-Hin(139–190) at 10 μm (Fig. 3, lanes 9 and 10). (**D**) Cleavage patterns for Fe · EDTA-Hin(139–190) at 1.5 μ*M* (Fig. 3, lanes 7 and 12). Extent of cleavage was determined by densitometric analysis of the gel autoradiogram.

ty cleaving data, footprinting of Hin(139–190) with methidiumpropyl-EDTA · Fe (MPE · Fe) was included (Fig. 3).

Histograms of MPE · Fe cleavage protection by Hin(139–190) cleavage sites and the Fe · EDTA-Hin(139–190) on a restriction fragment containing Hin binding sites are shown in Fig. 4. Two Hin(139–190) peptides bound the two half-sites occupied by Hin. The Fe · EDTA-Hin(139–190) produced two cleavage patterns on the symmetry axis side of the individual half-sites. EDTA-Hin(139–190) appears similar to the Hin(139–190) in that the two half-sites were not equally bound (*1*). The other major cleavage site (secondary Hin), which is also bound by Hin, is located just upstream from the initiation codon of the *hin* gene.

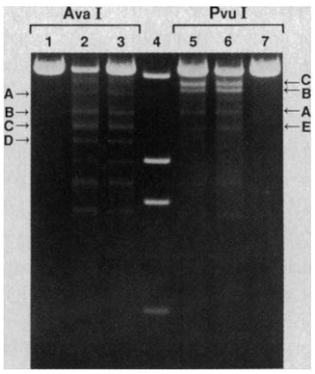

Fig. 5. Double strand cleavage from the reaction of Fe · EDTA-Hin(139–190) and linearized plasmid pMS515 (*22*) analyzed on a nondenaturing agarose gel. A to E are fragments that resulted from one double strand break at five sites on pMS515. Locations of double strand breaks with Eco RI defined as origin and the most probable recognition sequence 5′ to 3′ are: site A, 2479 (TTTTCTCCTTA); site B, 110 (*hix*L); site C, 3353 (TTATCAAAAA); site D, 4013 (TTCTGAGAAT); and site E, 2107 (TTATCAGAAG). Reaction conditions were 40 m*M* trisacetate, *p*H 7.9, 5 m*M* NaOAc, 5 m*M* DTT, 50 μ*M* (bp) DNA in a total volume of 10 μl, 1 hour, and 22°C. The products were separated on a 1% nondenaturing agarose gel with subsequent ethidium bromide staining. (Lanes 1 to 3) Ava I; (lanes 5 to 7) Pvu I linearized plasmid; (lane 4) molecular markers consisting of Rsa I and Eco RI digests of pBR322 (4363, 2118, 1565, and 680 bp). (Lanes 3 and 5) Fe · EDTA-Hin(139–190) at 10 μ*M* and (lanes 2 and 6) at 2 μ*M*; (lanes 1 and 7) DNA control lanes.

The cleavage patterns on opposite strands of DNA for Fe · EDTA-Hin(139–190) were shifted to the 3′ side at all binding sites (Fig. 4). This asymmetry reveals that the EDTA · Fe, and hence the NH_2-terminus of the peptide, is located in the minor groove of the DNA (Fig. 1). Positioning part of EDTA-Hin(139–190) in the minor groove is consistent with protection from methylation by the Hin(139–190) and Hin at A(−6), A(−5), A(−4) and A(4), A(5), A(6) of *hix*L (*1*).

The ability of Fe · EDTA-Hin(139–190) to cause double strand cleavage of DNA containing the *hix*L site was investigated. Double strand cleavage of linearized plasmid DNA containing the *hix*L site cloned into pBR322 is shown in Fig. 5. Fe · EDTA-Hin(139–190) at 5 and 10 μ*M* revealed two strong and three weak cleavage sites. One strong cleavage site mapped to the *hix*L site. The second strong site mapped to a location in pBR322 that is a perfect match to the outer 10 bp of the right half-site of *hix*L. The three weaker sites have lower degrees of sequence similarity to a *hix* half-site (Fig. 5). Identification of alternative DNA-binding sites for Hin(139–190) by gel electrophoresis is a useful feature of the affinity cleaving method for analyzing peptide:DNA recognition.

The cleavage data have demonstrated where the NH_2-terminal residue of peptide 1 is located with respect to the DNA-binding site. If Hin recognizes the binding site via specific contacts in the major groove, possibly with a helix-turn-helix structure, then the combination of the cleavage patterns of Fe · EDTA-Hin(139–190) and the footprinting results with Hin(139–190) indicates that the NH_2-terminal end of the peptide (Gly-Arg-Pro-Arg-) must extend across the DNA phosphodiester backbone and follow the minor groove toward the center of the dimeric binding site. The region C(−2)A(−1)A(1)G(2) at the center of a *hix* site may be where the recombination event occurs (*1*). The central 6 bp not bound by the 52-residue peptide would then be available to the recombination activity of the other ≈140 residues of Hin. Therefore, the positions that are contacted by Hin in the major grooves are separated by one turn of the DNA helix. A similar model for γδ-resolvase has been proposed (*18*). Furthermore, the COOH-terminal end of Hin contains several positive charges similar to the NH_2-terminal domain of λ-repressor which is believed to form an arm that wraps around DNA (*19*). The COOH-terminal region of Hin may be positioned to fulfill a similar role.

A binding model for the DNA recognition domain of Hin may involve three sets of interactions: (i) a helix-turn-helix structure binding at the outer 5 bp on both ends of a *hix* site (5′-TTCTT-3′ and 5′-TTATC-3′), (ii) a region that connects the helix-turn-helix domain with the other 140 residues of Hin by following the adjacent minor groove of sequence 5′-AAA-3′ toward the center of the *hix* site, and (iii) a COOH-terminal arm which follows the major groove. Two models that incorporate these features are shown in Fig. 6. The three α helices are based on the α_1-α_2-α_3 helices of cro (*2*) and 434 repressor (*5, 7*). The α_3 helix is placed in the major groove. The two models differ in the direction of the α_3 recognition helix relative to the direction along the major groove. For one model, the α_3 helix orientation is based on the 434 repressor cocrystal (*7*) and the other on the complex of *lac* repressor headpiece with a 14-bp *lac* operator fragment studied by two-dimensional nuclear magnetic resonance (*20*). It would seem that the helix-turn-helix motif may be necessary but not sufficient for binding in these systems. Binding may require a third α helix and structures that bind DNA in the minor groove to hold the DNA-binding helix-turn-helix domain in the proper configuration.

In summary, we have synthesized a 52–amino acid peptide equipped with EDTA at the NH_2-terminus. In the presence of Fe(II)

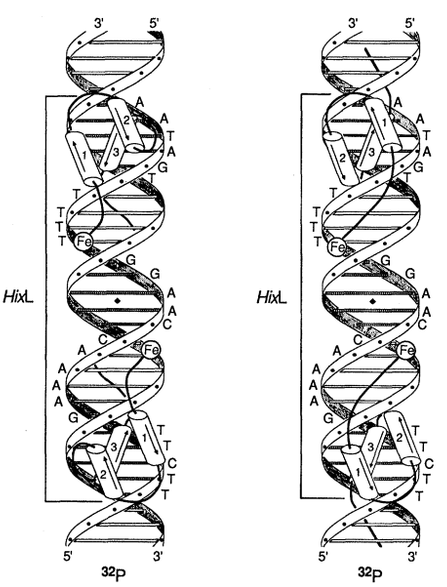

Fig. 6. Schematic representation of models for Fe · EDTA-Hin(139–190) and, by extension, the DNA recognition domain of Hin binding to *hix*L. The sequence of *hix*L is shown along the 5′ strand in the same direction as in Fig. 4. The pseudo C2 axis is marked by a solid diamond. Putative α helices (see Fig. 2A) are shown as cylinders with an arrow pointing from the NH_2- to the COOH-terminus. The model on the left is based on the 434 repressor fragment: 14-bp operator cocrystal (*7*) with the following changes; (i) 434 repressor α_4 helix is replaced with the ten-residue COOH-terminal tail of Hin, (ii) the nine-residue NH_2-terminal tail of EDTA-Hin(139–190), which includes EDTA, is added as an extension to the 434 repressor α_1 helix NH_2-terminus. The model on the right represents the recognition helix orientation of the *lac* repressor headpiece (*20*), which is rotated 180° from the 434 operator complex (*7*) and cro-OR3 model (*2*). This requires reorganization of the remaining helixes. The α_3 helix of *lac* repressor is replaced by the COOH-terminal tail of Hin. The orientation of the *lac* repressor α_1 helix (α_2 of EDTA-Hin(139–190)) is reversed so that the NH_2-terminus of the EDTA-Hin(139–190) α_1 helix is toward the pseudo C2 axis of *hix*L.

and reducing agents, EDTA-Hin(139–190) cleaves double-stranded DNA at the recognition sequence of the Hin recombinase site, revealing the location of the NH_2-terminus of Hin(139–190). The coupling of a DNA-binding peptide to a metal chelator creates a hybrid peptide capable of cleaving specific sites on DNA. Design of other multifunctional peptides capable of recognizing specific substrates and chemical modification of those substrates could lead to reagents for use in chemistry, molecular biology, and medicine.

REFERENCES AND NOTES

1. M. F. Bruist *et al.*, *Science* **235**, 777 (1987).
2. W. F. Anderson, D. H. Ohlendorf, Y. Takeda, B. W. Matthews, *Nature (London)* **290**, 754 (1981).
3. C. O. Pabo and M. Lewis, *ibid.* **298**, 443 (1982).
4. D. B. McKay and T. A. Steitz, *ibid.* **290**, 744 (1981); D. B. McKay, I. T. Weber, T. A. Steitz, *J. Biol. Chem.* **257**, 9518 (1982).
5. J. E. Anderson, M. Ptashne, S. C. Harrison, *Nature (London)* **316**, 596 (1985).
6. R. W. Schevitz *et al.*, *ibid.* **317**, 782 (1985).
7. J. E. Anderson *et al.*, *ibid.* **326**, 846 (1987).
8. D. H. Ohlendorf and B. W. Matthews, *Annu. Rev. Biophys. Bioeng.* **12**, 259 (1983).
9. C. O. Pabo, and R. T. Sauer, *Annu. Rev. Biochem.* **53**, 293 (1984).
10. The structure of the DNA–Eco RI endonuclease recognition complex provides an example of sequence-specific DNA-protein interaction that differs from the helix-turn-helix recognition motif [J. A. McClarin *et al.*, *Science* **234**, 1526 (1986)].
11. J. Zieg, M. Silverman, M. Hilmen, M. Simon, *ibid.* **196**, 170 (1977).
12. R. C. Johnson *et al.*, *Cold Spring Harbor Symp. Quant. Biol.* **49**, 751 (1984).
13. A. Glasgow and M. Simon, unpublished results.
14. R. P. Hertzberg and P. B. Dervan, *J. Am. Chem. Soc.* **104**, 313 (1982); R. P. Hertzberg and P. B. Dervan, *Biochemistry* **23**, 3934 (1984).
15. P. G. Schultz, J. S. Taylor, P. B. Dervan, *J. Am. Chem. Soc.* **104**, 6861 (1982); J. S. Taylor, P. G. Schultz, P. B. Dervan, *Tetrahedron* **40**, 457 (1984).
16. P. B. Dervan, *Science* **232**, 464 (1986).
17. R. B. Merrifield, *Adv. Enzymol.* **32**, 221 (1969).
18. S. S. Abdel-Meguid, N. D. F. Grindley, N. Smyth-Templeton, T. A. Steitz, *Proc. Natl. Acad. Sci. U.S.A.* **81**, 2001 (1984).
19. C. O. Pabo, W. Krovatin, A. Jeffrey, R. T. Sauer, *Nature (London)* **298**, 441 (1982).
20. R. Boelens, R. M. Scheek, J. H. van Bloom, R. Kaptein, *J. Mol. Biol.* **193**, 213–216 (1987).
21. J. Garnier, D. J. Osguthorpe, B. Robson, *J. Mol. Biol.* **120**, 97 (1978).
22. The plasmid pMS515 is pBR322 with a 150-bp insert containing *hix*L cloned in at the Cla I site.

23. We thank T. A. Steitz, S. B. H. Kent, and S. Mayo for helpful discussions. Supported by grants from the DARPA University Research Initiative Program, the National Foundation for Cancer Research, the NSF, NIH fellowship GM-09534-02 (M.F.B.), and a National Research Service Award (T32GM07616) from the National Institute of General Medical Sciences (J.P.S.).

15 May 1987; accepted 31 July 1987

YIGSR, a Synthetic Laminin Pentapeptide, Inhibits Experimental Metastasis Formation

YUKIHIDE IWAMOTO, FRANK A. ROBEY, JEANNETTE GRAF, MAKOTO SASAKI, HYNDA K. KLEINMAN, YOSHIHIKO YAMADA, GEORGE R. MARTIN

The invasion of tumor cells through basement membranes is a critical step in the formation of metastases. The binding of the malignant cells to laminin in the basement membranes allows their attachment and activates their invasiveness. Recently a synthetic nonapeptide from the B1 chain sequence of laminin was identified as a major site for cell binding. A pentapeptide within the nonapeptide sequence was found to reduce the formation of lung colonies in mice injected with melanoma cells and also to inhibit the invasiveness of the cells in vitro.

LAMININ, A BASEMENT MEMBRANE–specific glycoprotein, has various biological activities including promoting the attachment, growth, and differentiation of epithelial cells (*1*). It also appears to be involved in tumor cell invasion and metastasis. Malignant cells have more laminin on their surface, bind more laminin, and attach more readily to laminin (*2, 3*). Laminin increases their invasive and metastatic activity (*3, 4*) and induces the secretion of collagenase IV (*5*). These activities appear to involve the binding of laminin to a high affinity receptor on the cell surface (M_r = 67,000) (*6*), since proteolytic fragments of laminin ($M_r \cong$ 450,000) that bind to the receptor and block the formation of metastases (*4, 7*).

Laminin is composed of three chains, A(400 kD), B1(230 kD), and B2(220 kD) chain (*8*), which are arranged in a cross-shaped structure (Fig. 1). We have cloned and sequenced the B1 chain (*9*), prepared synthetic peptides and peptide-specific antibodies, and used these to identify a sequence (CDPGYIGSR) (*10*) in the B1 chain which is active in cell attachment, chemotaxis, and binding to the laminin receptor (*11*). In this report, we have tested the nonapeptide (called peptide 11) and its amide form (peptide 11–amide) as well as other peptides in (i) an in vitro invasion assay (*12*) and (ii) a murine model of lung tumor colonization after the intravenous injection of B16F10 melanoma cells (*13*). The in vitro invasion assay measures the ability of cells to attach, degrade, and migrate through a reconstituted basement membrane matrix. By means of this assay, invasiveness has been found to strongly correlate with metastatic activity (*12*). We find that peptide 11 and its terminal pentapeptide YIGSR inhibit tumor cell invasion. In other studies on cell adhesion and receptor binding, we found that peptide 11–amide was more active, probably because it neutralized the negative charge on the arginine (*14*). The amide form also appeared to be more active in the in vitro invasion assay (Fig. 2). Other peptides of 19 to 22 amino acids in length from different domains in the B1 chain of laminin (peptides 1-7 in Fig. 1) were inactive (Fig. 2; P2 is shown). Similar findings on the activity of the peptides were obtained in the in vivo assay for lung tumor colonization (Fig. 3). Both peptide 11 and peptide 11–amide reduced the numbers of lung tumors (by 74% and >90%, respectively) when administered with B16F10 cells by tail vein injection into mice (Fig. 3). The inhibition of colonization

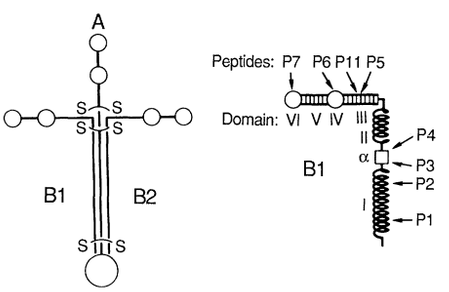

Fig. 1. Schematic model for the B1 chain of laminin. Seven structural domains in the B1 chain of laminin have been described and these are designated I–VI and α (*9*). The circles designate the globular regions of the laminin and the square designates an unusual cysteine-rich homologous repeat. P1 (residue 1593–1611), KQADEDIQGTQNLLTSIES; P2 (residue 1509–1529), KSGNASTPQQLQNLTEDIRER; P3 (residue 1395–1416), CRTDEGEKKCGGPGCGGLVTVA; P4 (residue 1363–1383), KLQSLDLSAAAQMTCGTPPGA; P5 (residue 960–978), NIDTTDPEACDKDTGRCLK; P6 (residue 615–634), KIPASSRCGNTVPDDDNQVV; P7 (residue 364–385), PERDIRDPNLCEPCTCDPAGSE; P11 (residue 925–933), CDPGYIGSR. Peptides were synthesized with an automated synthesizer, model 430 A (Applied Biosystems, Inc., Foster City, California). Their purity was checked by amino acid analyses and by high performance liquid chromatography.

Y. Iwamoto, J. Graf, M. Sasaki, H. K. Kleinman, Y. Yamada, G. R. Martin, Laboratory of Developmental Biology and Anomalies, National Institute of Drug Research, National Institutes of Health, Bethesda, MD 20892.

F. A. Robey, Bureau of Biologics, Food and Drug Administration, Bethesda, MD 20892.